01 Mar 2005

Hydrogeophysical Investigation at Luxor, Southern Egypt

Ahmed Ismail

Neil Lennart Anderson
Missouri University of Science and Technology, nanders@mst.edu

J. David Rogers
Missouri University of Science and Technology, rogersda@mst.edu

Recommended Citation

A. Ismail et al., "Hydrogeophysical Investigation at Luxor, Southern Egypt," *Journal of Environmental and Engineering Geophysics*, vol. 10, no. 1, pp. 35-49, Environmental and Engineering Geophysical Society (EEGS), Mar 2005.
The definitive version is available at https://doi.org/10.2113/JEEG10.1.35

Hydrogeophysical Investigation at Luxor, Southern Egypt

Ahmed Ismail[1], Neil L. Anderson[2] and J. David Rogers[3]
[1]National Research Institute of Astronomy and Geophysics,
Helwan, Cairo, Egypt
Email: aib57@umr.edu
[2]Department of Geology and Geophysics,
University of Missouri-Rolla, Rolla, Mo. 65401
Email: nanders@umr.edu
[3]Department of Geological Engineering,
University of Missouri-Rolla, Rolla, Mo. 65401
Email: rogersda@umr.edu

ABSTRACT

Over the past 35 years, the exposed stone foundations of the ancient Egyptian monuments at Luxor have deteriorated at an alarmingly accelerated rate. Accelerated deterioration is attributable to three principal factors: 1) excavation and exposure of foundation stone; 2) construction of the Aswan High Dam; and 3) changes in the regional groundwater regime. In an effort to better elucidate the hydrostratigraphy in the Luxor study area that extends from the River Nile to the boundaries of the Nile Valley and covers about 70 km^2, a geophysical/hydrological investigation was conducted. Forty Schlumberger vertical electrical soundings (VES), two approximately 6 km long seismic refraction profiles and a total number of 39 groundwater and surface water samples were acquired. Based on the integrated interpretation of the acquired geophysical/hydrological data, the main contributions of this study were the geophysical definition of the hydrostratigraphy using resistivity (seven distinct geologic/hydrologic units were mapped), the mapping of the water table using seismic refraction and the mapping of groundwater salinity trends through geochemical sampling. The factors contributing to the rise of groundwater and its accompanying increase in salinity were identified and documented. This characterization establishes a model for evaluating various plans to lower groundwater levels and salinities in the areas of archeological monuments.

Introduction

The east bank of Luxor (ancient city of Thebes) is famed for its archaeological heritage, which includes Luxor Temple, Madamod Temple and the Karnak Temple complex (Fig. 1). Most of these monuments are comprised of weakly silicified sandstones with high porosity (Said, 1981). After the decline of Egyptian empire, overbank deposits from the River Nile covered the foundations at Luxor Temple, Madamod Temple and the Karnak Temple complex. Until the mid-1980's, this sediment cover protected the stone foundations from wind abrasion, moisture loss and toppling effects (Sevi, 2002). Perhaps most importantly, capillary waters within the buried foundation stones did not rise above ground level except during brief periods of flooding.

In the mid Nineteenth Century, Luxor Temple, Madamod Temple and the Karnak Temple complex were excavated (to depths of several meters) by archeologists, and the foundation stone was exposed to the elements. In 1968, the Aswan High Dam was completed and seasonal fluctuations in the level of the River Nile were minimized. Discharge from the Aswan High Dam is now controlled to ensure that year-round navigation and year-round irrigation of the Nile's fertile floodplains is possible.

The control of the Nile's flow and related changes in the regional groundwater regime of the river's floodplain have wrought disastrous consequences on the structural integrity of the stone foundations of the ancient monuments in the Luxor area (Fig. 2), which date from between the 11th Dynasty (2081–1938 BC) and the 25th Dynasty (747–656 BC). The river's flow has been metered out by the Aswan High Dam since 1968, confining the river to its low flow channel. This control made year-round gravity-fed cropland irrigation possible and minimized seasonal fluctuations in the groundwater levels of the river's floodplain. As a result, groundwater levels are now elevated year-round. In addition, seasonal floods no longer remove accumulated salts, which are precipitated by evaporation from croplands under active irrigation. As a result, the salinity of capillary water has been greatly increased.

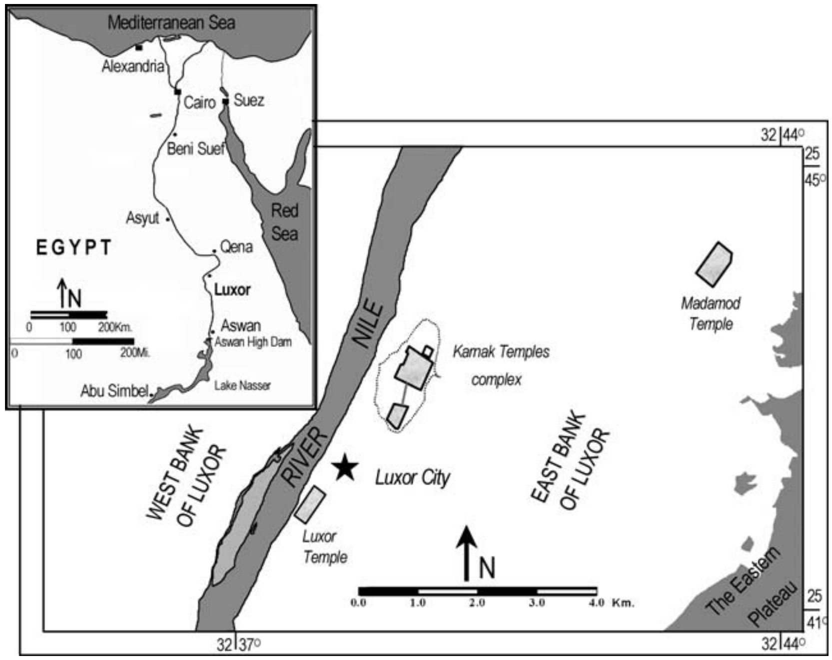

Figure 1. Luxor study area.

The excavation of the monument foundations has also contributed to the accelerated deterioration, as shown in Fig. 2. Prior to archeological excavation of up to three meters of encompassing soil, capillary waters within the foundation stones did not rise above the ground level except during peak flood periods. Now however, capillary water levels within the foundation stones are sustained at positive elevations with respect to the excavated ground surface. These capillary waters evaporate on the newly exposed surfaces of the foundation stonework. Pressure developed during crystallization and hydration of salts promotes exfoliation of the outer layers of the stone foundations, allowing more water to infiltrate the blocks and hasten their disintegration by wind and other physical processes (Lewin, 1982; Siebert *et al.,* 1984; Duttlinger and Knöfel, 1993; and Wüst and Schlüchter, 2000). Other factors, such as urbanization and the recharge of the Sacred Lake at Karnak Temple complex, may also serve to exacerbate the deterioration problem (Attia, 2001; Ismail, 2003).

Some efforts have been undertaken to mitigate the deterioration of the monument's masonry foundations, which are comprised of dressed sandstone. These efforts have focused mostly on technologies and/or processes which could lower groundwater levels and decrease groundwater salinity. Proposed/trial methodologies have included pumping groundwater from beneath the monuments, installing appropriate sanitary systems, and altering land use (Attia, 2001). These recent mitigation measures have not proven very effective, in part, because the hydrostratigraphy of the east bank of Luxor is not well documented nor understood.

Luxor Study Area

In an effort to understand the hydrostratigraphy of the east bank of Luxor, an integrated geological/geophysical/hydrological research study was conducted (Fig. 1). The study area extends from the River Nile (to the west) to the natural boundary of the Nile River Valley, which is highly dissected by a series of south-north flowing gravity-fed irrigation canals, constructed since 1968. The goals were to identify and map the different geoelectric (geologic/hydrologic) units in the shallow subsurface ($<$100 m), and determine the sources contributing to the rise in the level and the salinity of groundwater in the vicinity of monuments. It was thought that the results of the study would be of great use to those responsible for developing and implementing effective mitigation measures to retard further deterioration of the monuments.

Geologic And Hydrologic Overview

The study area is located on the alluvial plains of the Nile Valley, which are surrounded by elevated structural plateaus capped by Eocene age limestone and underlain by Paleocene age shale (Fig. 3). The alluvial plains in the study area slope gently to the north and east (from about 75.5 m amsl to about 79 m amsl; Fig. 4). These alluvial plains can be differentiated into a densely-cultivated younger plain occupying the central part of the Nile Valley and covered by Holocene silt and clay, and an older, reclaimed plain

Figure 2. Photograph of deteriorated stone foundation at the Karnak Temple complex.

covered by Pleistocene sand and gravel (El Hossary, 1994; RIGW, 1997; Fig. 4).

The near-surface Pliocene-Holocene sediments in the central part of the Nile Valley rest unconformably on a succession of Late Cretaceous to Early Eocene age marine sediments. The Pliocene-Holocene sediments have been subdivided into different units, each of which was deposited by an identified ancestral-modern river system, including the Eonile (Tmu), Paleonile (Tplu), Protonile (Q1), Prenile (Q2), and Neonile (Q3) river systems.

Two principal groundwater aquifers are distinguished within the Pliocene-Pleistocene units beneath Luxor (Fig. 4): the shallow Quaternary Aquifer, and the underlying Plio-Pleistocene Aquifer. The Quaternary Aquifer is comprised of graded sand and gravel with some clay and has a local thickness ranging from 5 to 95 m. This aquifer is semi-confined by an upper silty clay in the central part of the Nile Valley. However, the aquifer is phreatic where the silty clay layer thins, then terminates near the fringes of the river valley. The regional groundwater flow direction is east-to-west, towards the River Nile channel (El Hossary, 1994). The underlying Plio-Pleistocene Aquifer, comprised of sand, clay and gravel, represents the secondary aquifer in the study area. This aquifer is exposed near the Nile Valley fringe (Fig. 4). The salinity of the Plio-Pleistocene Aquifer is significantly higher than that of the overlying Quaternary Aquifer.

Geophysical and Hydrologic Data Overview

Resistivity data. The ground surface at Luxor study area is relatively flat and typically cultivated. The areas near the River Nile have been used for agriculture since ancient Egyptian time, while those closer to the outer edges of the Nile Valley are newly reclaimed land. Urbanization is generally either concentrated near the River Nile or the outer edges of the Nile Valley. The resistivity data were acquired in areas that are relatively free from cultural or geological noise.

Forty Schlumberger Vertical Electrical Soundings (VES) were acquired in the Luxor study area using a Syscal R2 resistivity system (Fig. 5). The Syscal R2 system measures and displays the current, the voltage, the standard deviation, and the apparent resistivity values. The system calculates apparent resistivity based on the type of electrode array and geometrical parameters that have been entered. Low pass analog filters reduce the effect of higher frequency natural and cultural noise. The system is powered by a 12 V external battery and has a maximum output power of 1600 W. The maximum current electrode spacing varied from 600 to

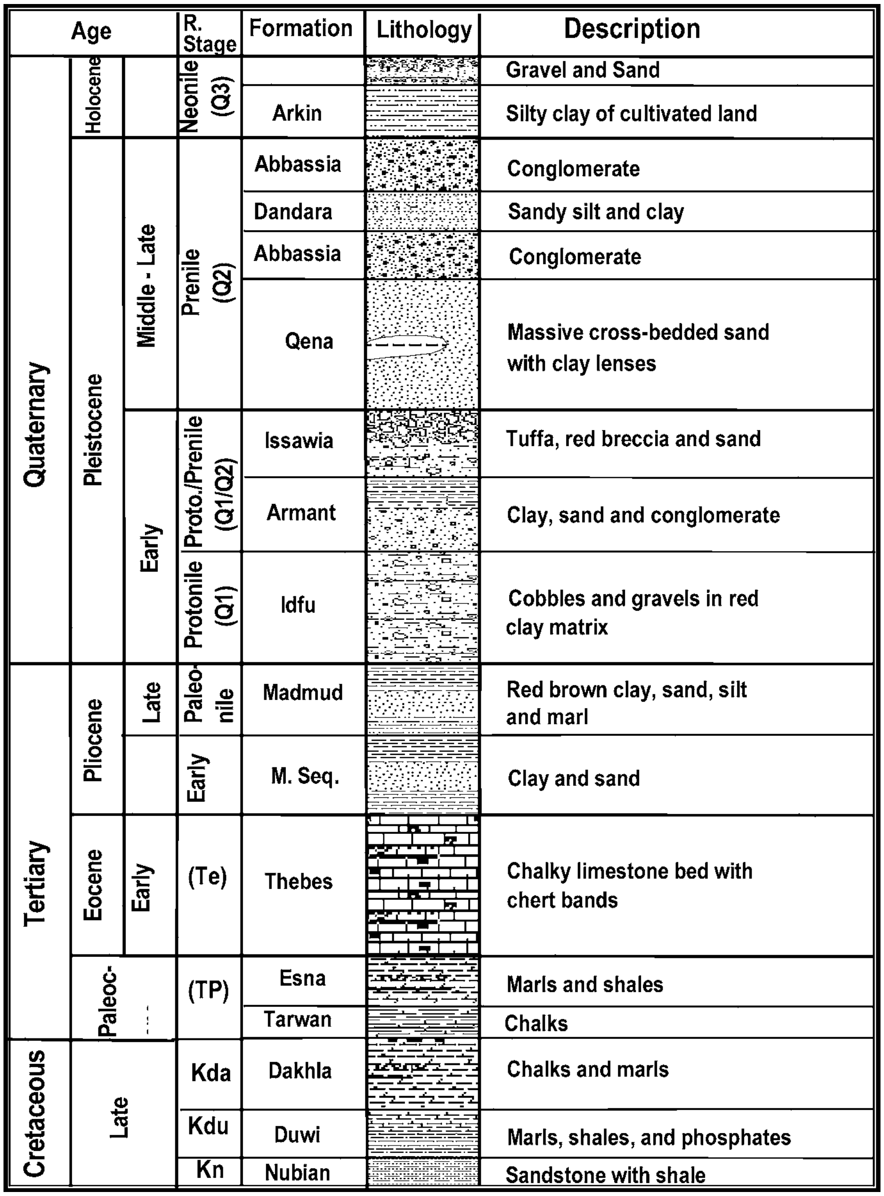

Figure 3. Composite stratigraphic column, Luxor study area (after El Hossary, 1994).

1,000 m as the AB/2 steps were 1, 1.4, 2, 3, 4, 6, 8, 10, 14, 20, 30, 40, 60, 80, 100, 140, 200, 300, 400 and 500 m. The distances between the potential electrodes were increased only few times and in relatively small steps (from 0.8 to 20 m) in order to obtain measurable potential differences. The distance between the centers of adjacent soundings was generally 1 to 3 km. Eight of the acquired soundings were conducted near existing boreholes where subsurface control was available.

The acquired resistivity data were inverted and interpreted in order to identify the different geoelectric units in the study area. ''True'' unit resistivities and thicknesses were also estimated. Three different automated inversion software programs were tested [Zohdy and Bisdorf, 1989; SCHLINV (Merrick, 1977) modified by Sauck, 1990; and Meju, 1992].

The interpretation procedures in the automatic computer program of Zohdy and Bisdorf (1989) are based on obtaining true depths and resistivities from shifted current electrode spacings and adjusted apparent resistivities, respectively. The method is fully automated and does not require an initial guess of the number of layers, their thickness or their resistivities. However the number of layers in the obtained model equals the number of digitized points on the sounding curve.

The results obtained from Zohdy and Bisdorf (1989) program were used to build a starting model for the automated inversion program developed by SCHLINV

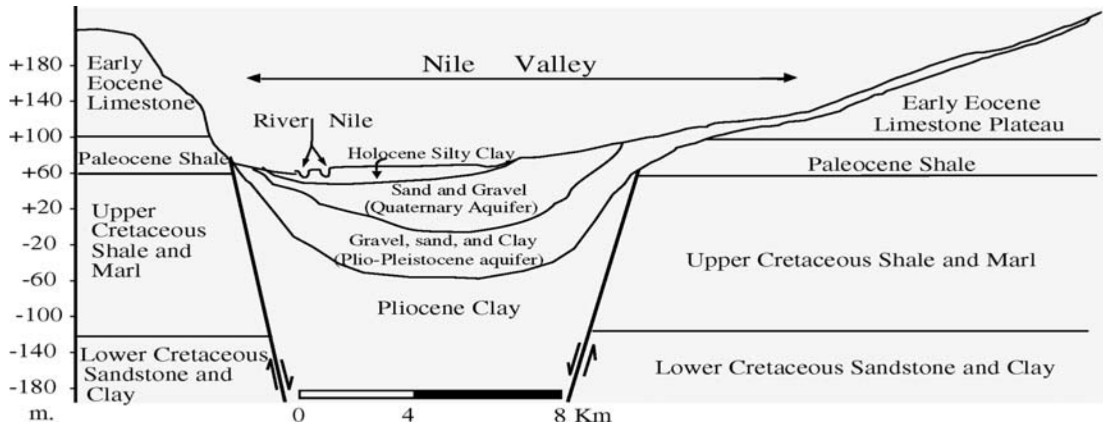

Figure 4. Hydro-geologic cross-section at Luxor area (RIGW, 1997). The valley is a structurally controlled graben with opposing faults.

(Merrick, 1977 modified by Sauck, 1990). In this interpretation procedure, a linear filter theory, coupled with the Marquardt method, automatically interprets the resistivity sounding data. The match between the field and model data (goodness of fit) is measured by the sum of squares of logarithms of the field and model data.

The automatic computer program developed by Meju (1992) was used to interpret the resistivity data. This program uses a Ridge regression procedure for inversion of the resistivity sounding data. In this program, the corrections to the initial model are damped to stabilize the inversion. Starting with a large positive damping factor ensures that the good initial convergence characteristics of the steepest descent method dominate. Damping decreases after each iteration to hasten the convergence to the proper solution. The two-stages minimization procedure incorporated in the algorithm adopted in Meju's program ensures meaningful results for a wide range of initial models.

The resistivity-depth models of many VES obtained from the three-inversion programs were compared with borehole controls in the study area. It was found that the Meju inversion program provide a more accurate resistivity-depth model than the other two programs. Consequently, the inversion results of Meju's program were used for data interpretation.

The resistivity data interpretations were used to

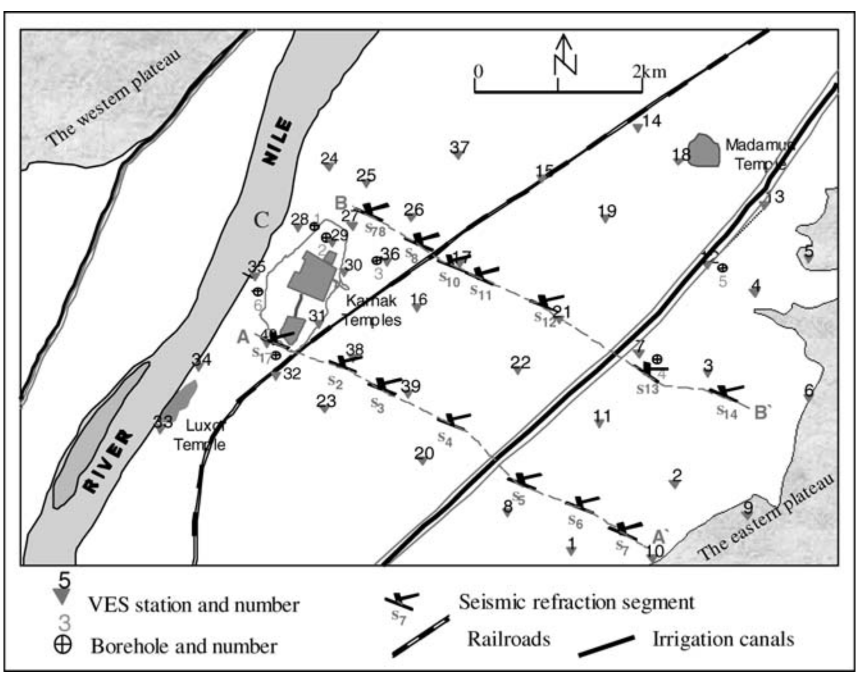

Figure 5. Locations of resistivity and seismic refraction.

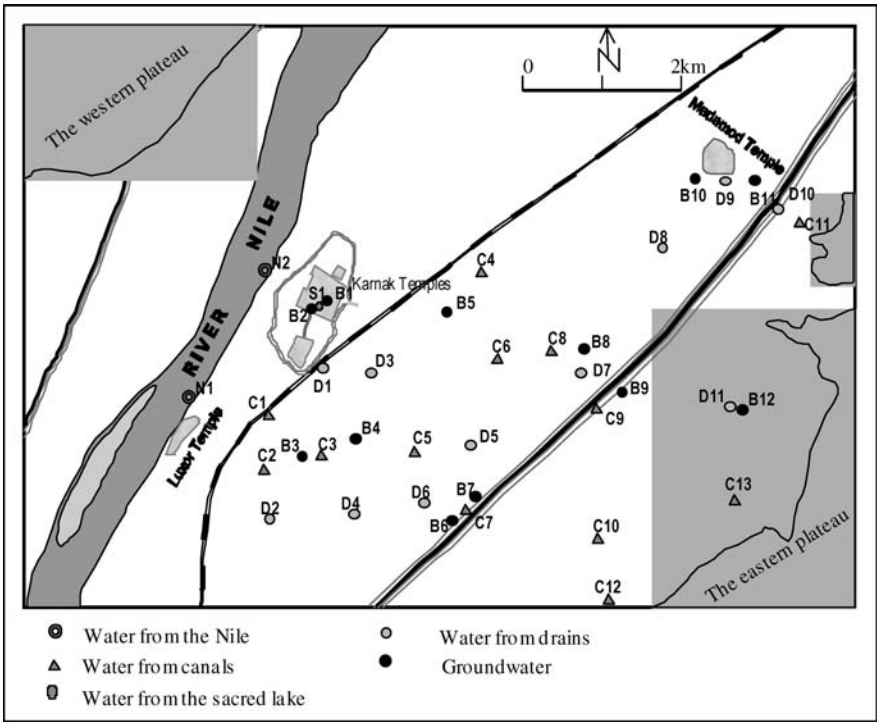

Figure 6. Location map of the collected groundwater and surface water from Luxor study area.

generate a suite of geoelectric resistivity cross-sections and subsurface resistivity/thickness maps. These sections and maps were analyzed to characterize the geologic/hydrologic units in the shallow subsurface (<100 m) in the study area.

Seismic refraction data. Refraction seismic control was acquired along two approximately 6-km long profiles in the Luxor study area using a Geometrics Strata View portable seismograph with 48 input/output 14 Hz geophones (Fig. 5). The geophones were spaced at 2-m intervals providing a spread length of 96 m. Two in-line spreads were acquired at each location. Forward- and reverse-direction shots were applied at offset of 2 m from each end of the array. This was to provide sufficient data along each spread to map changes in the subsurface parameters with confidence. A hammer on striker plate was used as a source during data acquisition and the resulting signal was stacked 10 to 20 times on the seismograph.

The two spreads at each location were analyzed together and transformed into seismic velocity profiles using SIP automated software (Rimrock Geophysics, 1995), which typically provides depth estimates to the seismic refractor beneath each geophone. The SIP program uses inverse modeling and iterative ray tracing techniques. The inversion algorithm uses the delay-time method to obtain a first approximation depth model, which is then trimmed up by a series of ray-tracing and model-adjustment iterations that seek to minimize the discrepancies between the field-measured arrival times and the corresponding times traced through the cross-sectional depth model.

Interpretation of the seismic refraction data was constrained by subsurface control from the existing boreholes and resistivity control. The interpretation of seismic refraction data helped to determine depths to the top of the fully saturated zone and to subsequently estimate the groundwater flow directions in the study area.

Hydrological data. A total of 39 groundwater and surface water samples were collected in the Luxor area for physical and chemical analysis (Fig. 6). The sources of the water samples include: two samples ($\mathbf{N_1}$ and $\mathbf{N_2}$) from the River Nile; thirteen samples ($\mathbf{C_1}$ to $\mathbf{C_{13}}$) from the canals; eleven samples ($\mathbf{D_1}$ to $\mathbf{D_{11}}$) from the drains; one sample ($\mathbf{S_1}$) from the Scared Lake of the Karnak Temple complex; and twelve groundwater samples ($\mathbf{B_1}$ to $\mathbf{B_{12}}$) from depths ranging from 5 to 35 m.

Surface water was grab-sampled from the River Nile, canals, drains, and the Sacred Lake of the Karnak Temple complex. The groundwater (Quaternary Aquifer water) was sampled either from hand pumps attached to water wells or from existing piezometers. To ensure the removal of stagnant water in the water well hand pumps, the temperature and specific conductance were monitored while pumping. When these parameters stabilized, indicating delivery of in situ water from the formation, water samples were collected. The total dissolved salts (TDS) as well as concentrations of the

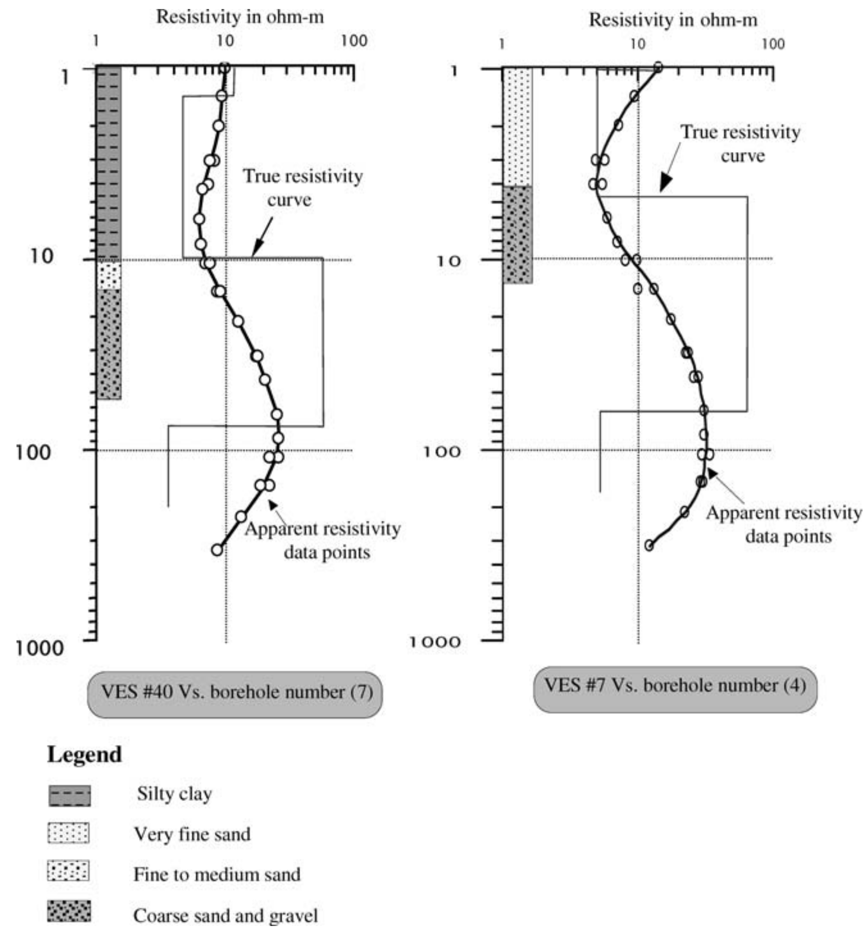

Figure 7. Comparison of the "true" resistivity from VES #40 with the lithologic control from borehole #7 (a) and "true" resistivity from VES #7 with the lithologic control from borehole #4 (b).

major ions were measured. These data were used to determine the salinity distribution within the Quaternary Aquifer water in the study area and the interrelationship between surface water and groundwater.

Data Interpretation and Significance

Resistivity data. Initially, the true resistivity curves (for eight VES) were compared with lithologic control from the adjacent boreholes (Fig. 7). These comparisons showed that relatively high resistivities ($\sim$20 Ω-m) characterize the upper relatively dry silty clay; relatively low resistivities ($\sim$4 Ω-m) characterize the moist silty clay; and significantly higher resistivities ($\sim$50 Ω-m) characterize the graded sand and gravel of the Quaternary Aquifer. The fourth geoelectric unit (characterized by low resistivities; $<$10 Ω-m) is depicted on the true resistivity curves at depths greater than those of the boreholes. This deeper unit is probably within the Plio-Pleistocene Aquifer (sand, clay, silt and gravel; based on available geological/hydrological control).

On the basis of the interpretation of the individual VES and the ''true'' resistivity/lithologic correlation, ten-geoelectric resistivity cross-sections were generated; four of these sections and their locations are shown in Fig. 8. The geoelectric resistivity cross-section parallel to the River Nile (Figs. 8b, c) shows four geoelectric units with no significant lateral variation of resistivity within the individual units. In the direction perpendicular to the River Nile, the shallow subsurface was characterized by seven geoelectric units (Figs. 8d, e), which include: a relatively dry topsoil; a moist silty clay; sand and gravel of the Quaternary Aquifer; sand and clay of the Plio-Pleistocene Aquifer; fine sand and silt of the newly reclaimed land; sand and gravel of the non-cultivated land; and limestone of the foot of the eastern plateau.

The shallowest geoelectric unit (assigned to the relatively dry silty clay) was characterized by higher resistivity than that of the lower moist silty clay. This difference in resistivity is due to capillary water increasing the moisture content of the lower moist silty clay. Accordingly, the interface between the two units (located at an average depth of 1.5 m) probably reflects the upper limit of the capillary water

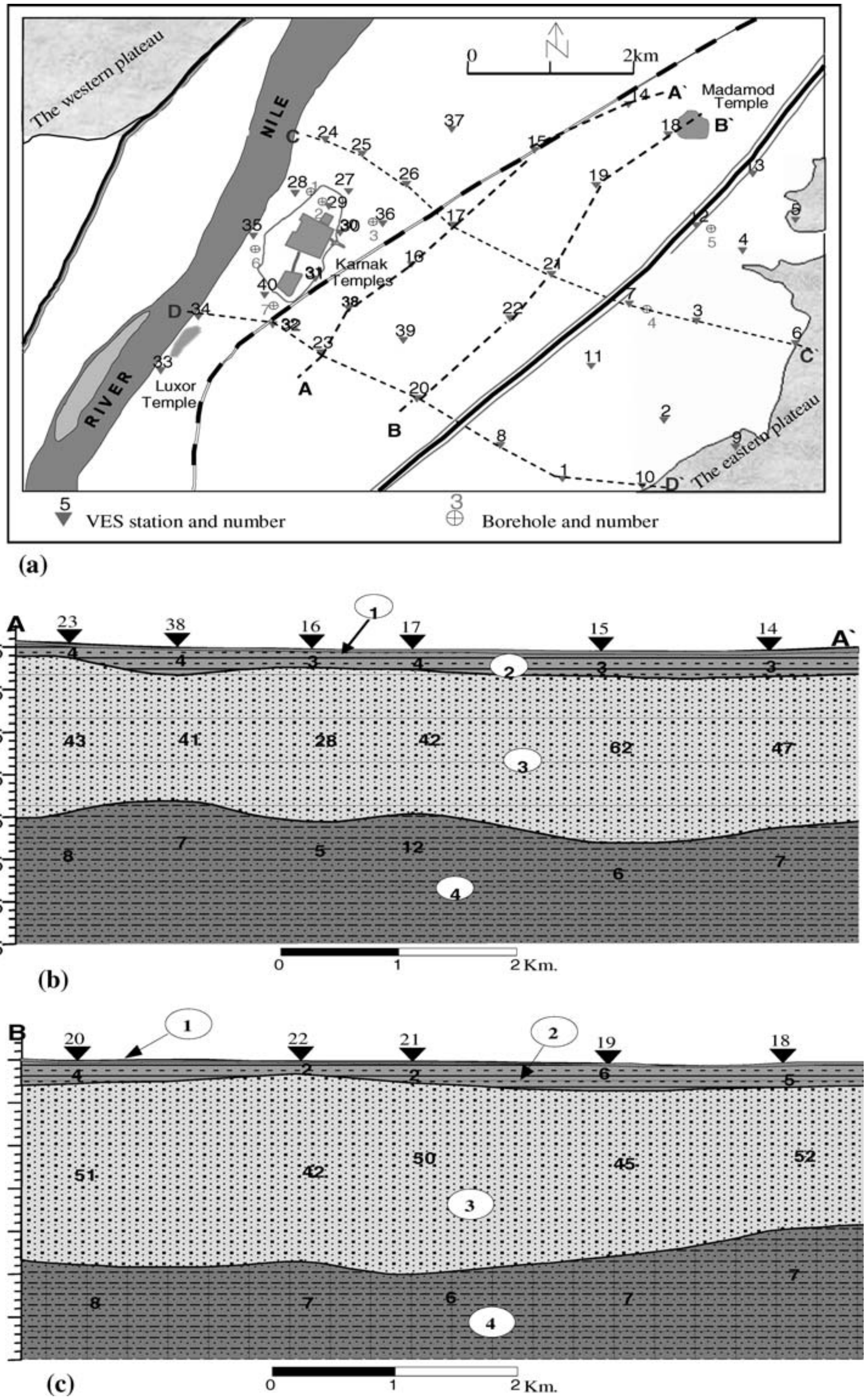

Figure 8. Geoelectric cross-sections at Luxor study area: (a) a map showing the locations of the cross-sections; (b and c) geoelectric cross-sections parallel to the river Nile; (d and e) geoelectric cross-sections perpendicular to the River Nile.

in the study area. The upper limit is much higher now than it was before the Aswan High Dam was completed in 1968.

The thickness and resistivity of the four geoelectric units imaged in Figs. 8b, c were mapped, however only the thickness of the second unit (moist silty clay) and the resistivity of the third unit (Quaternary Aquifer) are discussed here. The thickness of the second geoelectric unit generally increases towards the River Nile, and thins and

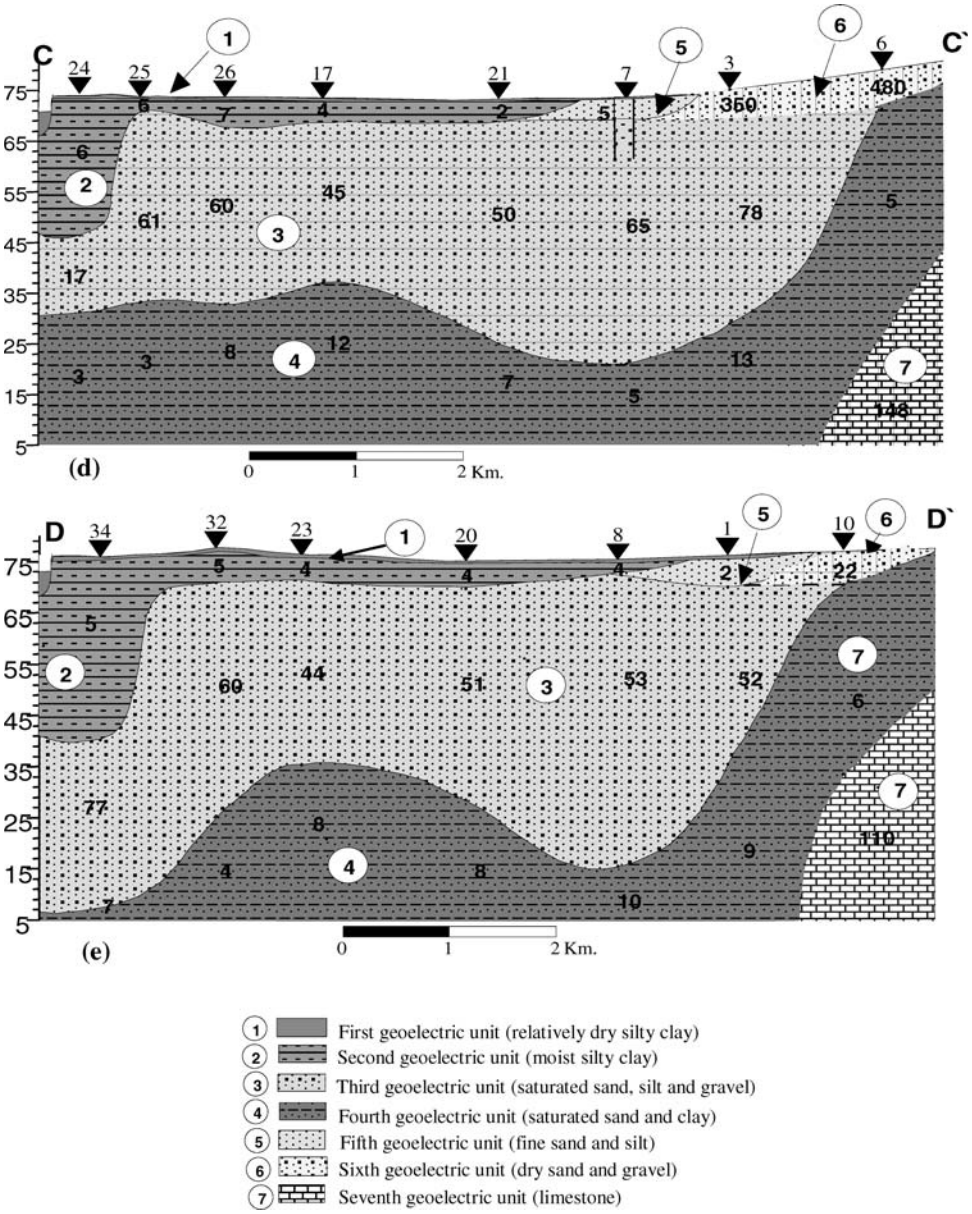

Figure 8. (Continued.)

pinches out eastward (Figs. 8 and 9). However, this unit is anomalously thicker (12 to 28 m) underneath the area of Karnak and Luxor Temples, where it may have been deposited in a paleo-meander of the River Nile. This anomaly is significant and must affect the local hydrologic environment. This could include reducing the potential rise of capillary water, decreasing the rate of lateral flow of groundwater, reducing the vertical drainage of surface water and increasing the salinity in vicinity of the paleo-meander.

The third geoelectric unit is characterized by relatively high resistivity (17 to 95 Ω-m; Figs. 8 and 10) and significant thickness (10 to 60 m). It represents the sand, silt and gravels forming the Quaternary Aquifer in the study area. This geoelectric unit exhibits significantly higher resistivity than the overlying silty clay and underlying sand and clay of the Plio-Pleistocene Aquifer. These resistivity contrasts allowed for the determination of the thickness and resistivity of the unit. Resistivity values within the third unit generally decrease toward the River Nile. This decrease in resistivity could be caused by a general increase in the groundwater salinity in this direction and/or lateral lithologic changes. However the increase in the groundwater salinity towards the River Nile, as inferred by the geochemical analysis, is consistent with the decrease in resistivity in the same direction.

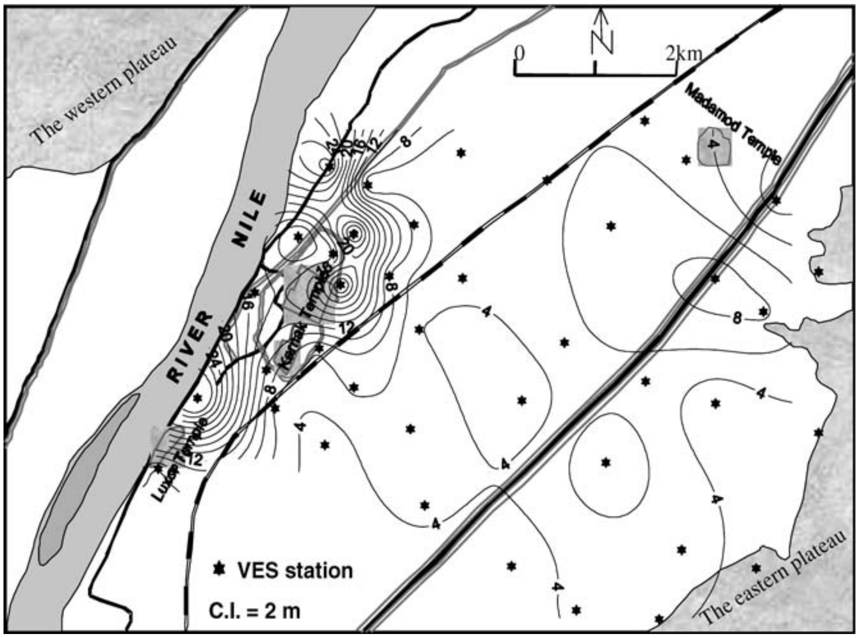

Figure 9. Isopach map of the second geo-electric unit (moist silty clay), Luxor study area.

Seismic refraction data. Borehole lithological control was used to constrain interpretation of the seismic refraction data (Fig. 11). At borehole number 4 an abrupt seismic velocity increase was observed in the data plot and the interpretation (Figs. 11a, b). The abrupt seismic velocity increase was associated with the position of the absolute groundwater table (zone of complete saturation) within the sand and gravel layer (Fig. 11b). At borehole number 2 a seismic velocity increase was observed within the silty clay layer (Figs. 11c, d). Based on the change in seismic velocity, the silty clay layer was subdivided into two seismic layers (Fig. 11d): an upper seismic layer with a low seismic velocity of 466 m/s and a lower seismic layer with a velocity of 1,528 m/s (higher than the compressional wave velocity of water).

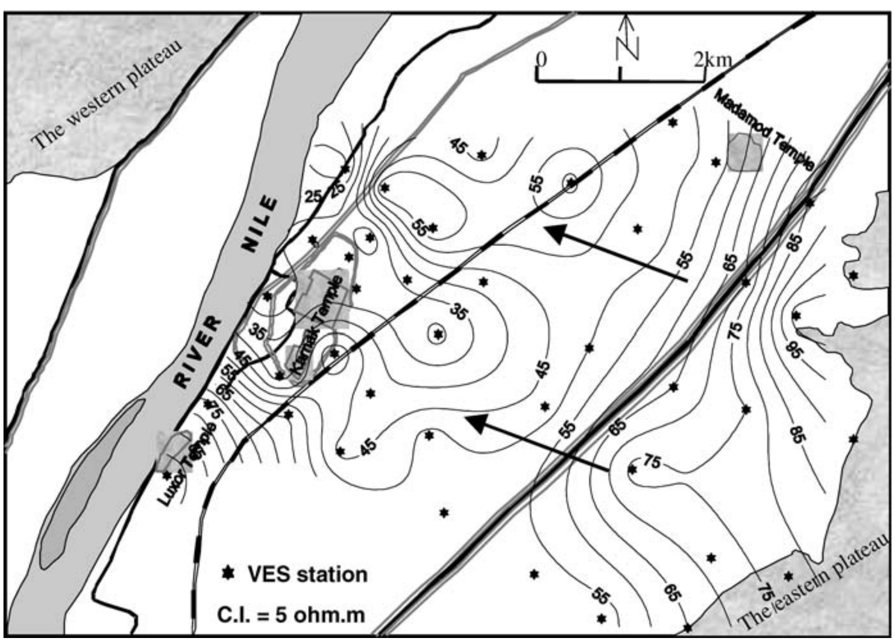

Figure 10. Resistivity map of the third geoelectric unit (graded sand and gravel of the Quaternary Aquifer), with the arrows showing the general trend of decreasing resistivity towards the River Nile in Luxor study area.

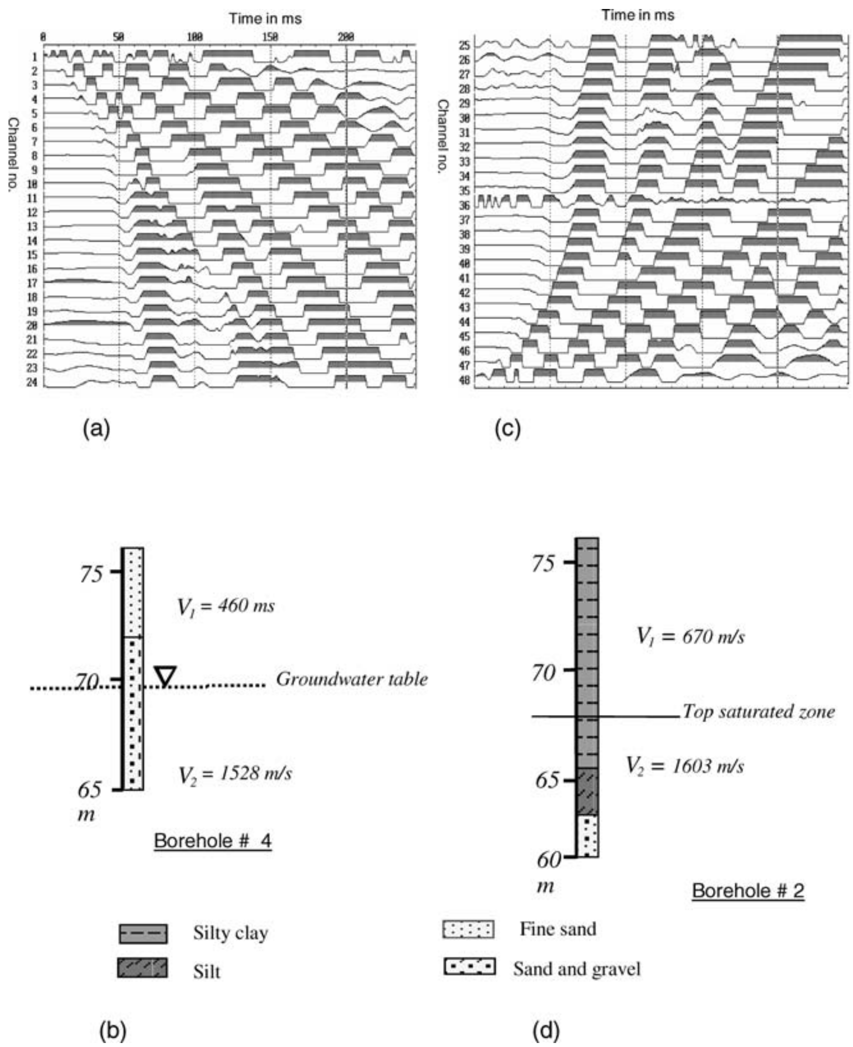

Figure 11. (a) Seismic refraction data plot acquired nearby borehole # 4; (b) seismic velocity compared with borehole # 4; (c) seismic refraction data plot acquired nearby borehole # 2; and (d) seismic velocity compared with borehole #2. Vertical scale is elevation above sea level (amsl).

Comparison of the seismic velocities with the subsurface controls indicates that the boundary between the two imaged seismic layers is most likely the zone of complete saturation (groundwater table) rather than a lithologic change. This conclusion is consistent with the conclusion of Murphy *et al.* (1993), Schön (1996) and Domenico (1977) who state that a sharp decrease in the seismic velocity occurs with a small decrease from 100% water saturation in porous sands.

Based on the interpretation of the acquired seismic refraction data and borehole control, the shallow subsurface (<20 m) can be subdivided into two seismic velocity layers: 1) the first (upper) seismic layer has a relatively low seismic velocity ranging from 390 to 750 m/s and thickness ranging from 3 to 9 m. This layer corresponds to the dry to partially saturated soil in the study area; and 2) the second seismic layer has a relatively high seismic velocity of >1,500 m/s and corresponds to the completely saturated soil zone.

The estimated depths to the interface between the two seismic velocity layers were used to construct a contour map of the elevation of the top of the saturated zone (Fig. 12). This map showed that the top of the saturated zone is relatively high (72.5 m amsl, 3 m below the surface) in the central part of the study area and declines gently eastward and westward to reach an average elevation of 68.5 m amsl (9 m below the surface). Consequently, the groundwater flow direction can be estimated to be from the central part of the study area eastward and westward. Moreover, the eastern part of the study area at Karnak and Luxor Temples showed relatively steep hydraulic gradient within the silty clay layer, which would be expected of a material with a lower hydraulic conductivity.

Hydrological data. Analysis of the groundwater and surface water samples (TDS and concentrations of the major ions) showed that, the salinity of the River Nile water in the

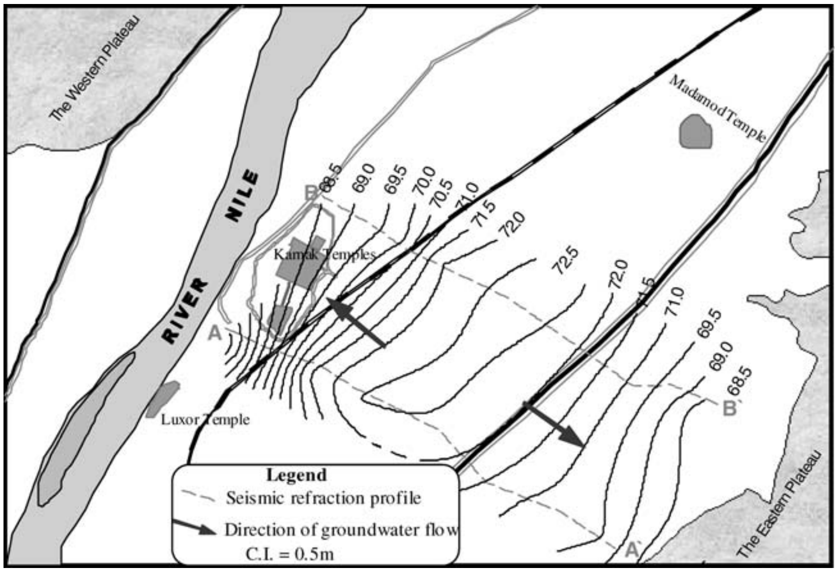

Figure 12. Contour map of the elevation (in meters amsl) of top of the fully saturated zone, Luxor study area, based on interpretation of seismic refraction data.

study area is 173 mg/L, the canal water averages 280 mg/L, while water in the drains averages 426 mg/L. The TDS of water in the Sacred Lake of the Karnak Temple complex is relatively high (780 mg/L). The relatively high TDS of surface water in canal/drain network and in the Sacred Lake may be influenced by the surface activities, lack of precipitation and excessive evaporation from the hot, dry climate. Groundwater salinity ranges from 524 mg/L to 1,363 mg/L, increasing from the edges of the Quaternary Aquifer towards the River Nile in the same direction as the groundwater flow (Fig. 13). The maximum salinity measured in the groundwater occurs beneath the Karnak and Madmod Temples (1,200 mg/L and 1,100 mg/L respectively). The high salinity beneath the temples may be attributed to: 1) a general absence of leaching by infiltrating rainwater because of the cover afforded by the temples themselves; 2) the evaporation of surface water in Luxor and flushing of residual high salinity water into the subsurface; 3) poor drainage in the areas underlain by the low permeability silty clay may increase the groundwater salinity in the shallow subsurface;

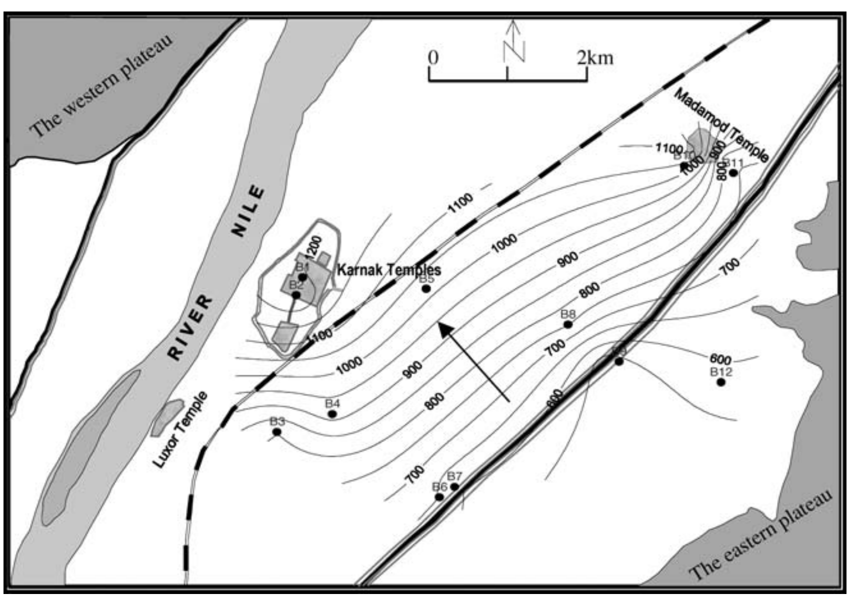

Figure 13. Iso-salinity contour map of groundwater in Quaternary Aquifer, Luxor study area.

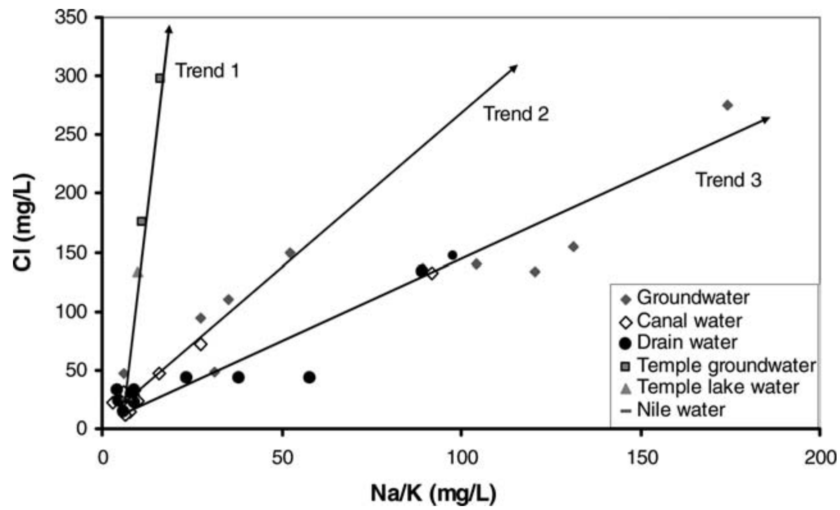

Figure 14. Cross plot of Na/K ionic concentration and Cl ion concentration.

and/or 4) the leaching of salts from nearby fields under cultivation and/or sewage from the urbanized areas where the silty clay is thin may progressively increase the salinity of groundwater along its flow path towards the River Nile.

The Na/K ionic concentration was plotted versus the chloride ion concentration for the entire sample set (Fig. 14) to compare the surface water and groundwater chemistry. This plot shows that the water from the Sacred Lake (S1) and the groundwater underneath the temples (B_1 and B_2) exhibit similar trend (trend 1) of relatively high chloride concentration. This trend shows a relatively higher concentration of K indicating processes (rock-water interaction) of local origin. This suggests that the Sacred Lake water, which exhibits higher evaporation rates (because it is surrounded by hardened surfaces that reflect the sun's energy), may serve as the primary recharge source for groundwater beneath the temples. Trend 3 in Fig. 14 shows a relatively lower concentration of K which represents water samples of the origin similar to the Nile water. Trend 2 represents water samples which are perhaps mixture from both trends water samples.

Discussion

Three significant observations have been noted with respect to the interpretation of the geophysical and hydrologic data: 1) there is an abrupt increase in the thickness of the silty clay unit in the vicinity of the Karnak and Luxor Temples (likely an old channel fill); 2) groundwater flows from the reclaimed agricultural land towards the temples and the River Nile; and 3) groundwater salinity increases from east to west towards the temples and the River Nile.

An unexpected finding was the discovery of an anomalously thick deposit of silty clay (~28 m) in vicinity

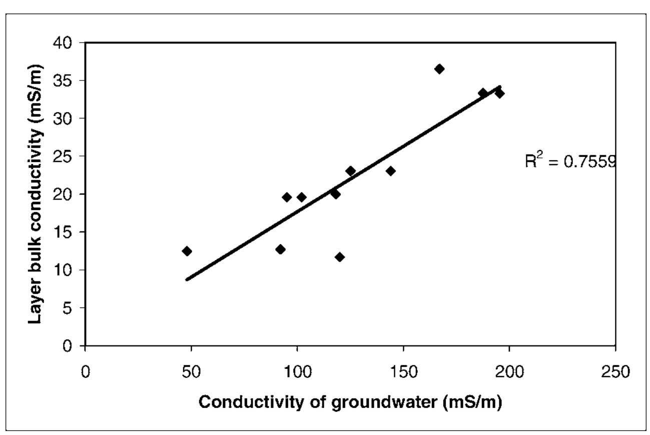

Figure 15. Bulk conductivities of geoelectric layer 3 (the Quarternary Aquifer) at various VES survey locations plotted against the conductivities of groundwaters sampled at those same locations.

of the temples. This crescent shaped deposit appears to be a paleo-meander of the River Nile. If it was pinched off as a quasi-oxbow meander, the paleochannel deposit should exhibit higher salinity than the materials bordering it, because the connate water would have become progressively saline as the oxbow evaporated. Thus, salts trapped within the silty clay could also be contributing to the increased salinity beneath the temples. An alternative explanation may be that the large plug of silty clay acts as a groundwater percolation barrier promoting increased runoff infiltration into the more pervious materials bordering the old channel fill. Some of this percolation must also originate from the year-round irrigation of the gardens surrounding the temples. The silty clay plug might also increase lateral capillary flow from septic-tanks (built after 1968) toward the topographic lowland occupied by the temples. The high rate of evaporation at Luxor would also increase salt concentrations in the residual surface water and shallow groundwater around the old city. Collectively, these factors probably explain the high salinity of the Sacred Lake water (780 mg/L) as well as the extremely high chloride concentration (3,642 mg/L) in the shallow groundwater ($<$1 m depth) recorded by Sevi (2002) at a test site just a few meters from the Karnak Temple complex.

The flow of groundwater towards the temples, as determined from the interpretation of seismic refraction data (Fig. 12), is consistent with determinations in previous studies (RIGW, 1997). This flow is likely the principal factor promoting the observed rise in groundwater levels in the area of the Luxor temples. The potentiometric head promoting this flow appears to be recharge emanating from newly-irrigated fields situated higher on the Nile floodplain, east of Luxor.

Groundwater salinity increased from the Nile Valley fringes towards the River Nile (Fig. 13). This salinity increase occurs in the direction of observed groundwater flow, reaching its maximum beneath the Karnak and Madmod Temples. This observation contrasts with previous studies (El Hossary, 1994) which concluded that salinity increased with distance from River Nile towards the valley fringes. The surprising increase in groundwater salinity beneath the temples may be due to a variety of factors, including the leaching of agricultural chemicals and/or sewage from urban areas.

The groundwater flow path and noted salinity variations are characteristic of the saturated zone. However, in most cases, the deteriorating monuments at Luxor are not in direct contact with the saturated zone. Flow in the saturated zone brings water and salts to the area beneath the monuments, but the saline mixture is lifted upward through several mechanisms. These mechanisms appear to include capillary action, thermo-migration of water and desiccation.

It was noted that the increase in groundwater salinity is generally consistent with the decrease in the inferred resistivity of the Quaternary Aquifer layer (Figs. 10 and 13). Figure 15 shows an almost linear relationship between groundwater electrical conductivity (chiefly a function of salinity) and layer's bulk conductivity (reciprocal of resistivity). Such linear relationship suggests that the layer bulk conductivity is tied to the groundwater salinity across the study area. More specifically, the observed decrease in resistivity towards the River Nile is likely due to the increase in groundwater salinity rather than variations in lithology. Accordingly, the resistivity of the Quaternary Aquifer layer inferred from a VES survey can be used to predict gross variations in the groundwater salinity, particularly in areas where drilling boreholes is prohibited because of the underlying antiquities.

Conclusions

Herein, the shallow subsurface in the Luxor study area is subdivided into seven distinct geologic/hydrologic units. Such characterization represents the foundation of any plan to lower the groundwater and decrease the salinity capillary soil moisture in the area of the Luxor monuments. Shallow groundwater flow paths were traced to originate from the recently-cultivated areas east of Luxor towards the River Nile, elevating the groundwater table beneath the ancient temples. This rise of the water table was accompanied by a marked increase in groundwater salinity along the same flow path, with the maximum concentrations beneath the temples.

The elevated groundwater at the area of the temples appears attributable to flood irrigation of recently reclaimed lands lying on the alluivial/flood plain transition, several kilometers east and a few meters above old Luxor. The progressive increase in groundwater salinity along the flow path is being reflected in the recent deposition of precipitated salts observed on the temple foundations. The Sacred Lake of the Karnak Temple complex probably worsens the situation by recharging the groundwater table beneath the temples. Based on the accumulated data it would appear that the salt accumulation on the foundations of the monuments is ascribable to salt transport by capillary water from the relatively high salinity groundwater or connate water in the thick silty clay unit.

References

Attia, F., 2001, Causes of high groundwater in antiquity sites and possible prevention/remedial measures: Proceedings of the workshop on groundwater impacts on antiquities, Luxor, Egypt, May 16–17.

Domenico, S., 1977, Elastic properties of unconsolidated sand reservoirs: Geophysics, **42**, 1339–1368.

Duttlinger, W., and Knöfel, D., 1993, Salzkristallisation und Salzschadensmechanismen *in* Jahresberichte Steinzerfall:

Steinkonservierung, Snethlage, R. (ed.), Ernst & Sohn, Berlin, 197–213.

El Hosary, M., 1994, Hydrogeological and hydrochemical studies on Luxor area, southern Egypt: B.Sc. thesis, Faulty of Science, Ain Shams University, Cairo, Egypt.

Ismail, A., 2003, Geophysical, hydrological and archaeological investigation in the east bank area of Luxor–Southern Egypt: Ph.D. thesis, University of Missouri-Rolla, Rolla, Missouri, USA.

Lewin, S., 1982, The mechanism of masonry decay through crystallization: in Conservation of historic stone buildings and monuments: National Academy Press, Washington, 120–144.

Meju, A., 1992, An effective ridge regression procedure for resistivity data inversion: Computers and Geoscience, **18**, 99–118.

Merrick, P., 1977, A computer program for the inversion of Schlumberger sounding curves in the apparent resistivity domain: Hydrogeological Report #197715, Water Resources Commission: N.S.W., Australia.

Murphy, W., Reischer, A., and Hsu, K., 1993, Modulus decomposition of compressional and shear velocities in sand bodies: Geophysics, **58**, 227–239.

RIGW (Research Institute of Groundwater), 1997, Hydrogeological map of Luxor area: Scale 1:100 000. Explanatory notes.

Rimrock Geophysics, 1995, User's manual guide to SIPx programs.

Said, R., 1981, The geological evolution of the River Nile: Springer-Verlag, NewYork.

Sauck, W., 1990, Modification of the SCHLINV (Merrick, 1977) program: Internal report, Institute for Water Sciences, Western Michigan University, Kalamazoo, Michigan.

Schön, H., 1996, Physical properties of rocks: Handbook of geophysical exploration: Pergamon Press, Oxford, UK.

Sevi, A., 2002, Deterioration of stone foundation of antiquities at Luxor-Egypt: M.Sc. thesis, University of Missouri-Rolla, Rolla, Missouri.

Siebert, R., Moncure, G., and Lahann, R., 1984, A theory of framework grain dissolution in sandstones: *in* Clastic diagenesis, McDonald and Surdameds (eds.), AAPG Memoir 37, 163–175.

Wüst, and Schlüchter, C., 2000, The origin of soluble salts in rocks of the Thebes Mountains, Egypt: The damage potential to ancient Egyptian wall art: Journal of Archaeological Science, **27**, 1161–1172.

Zohdy, A., and Bisdorf, R., 1989, Programs for the automatic processing and interpretation of Schlumberger sounding curves in QuickBASIC 4.0: U.S. Geological Survey, Open-File Report, 89–137.